On the extraction of power-law tails of the probability density functions in star-forming clouds

Lyubov Marinkova[1], Todor Veltchev[1], Orlin Stanchev[1], Sava Donkov[2]
[1] University of Sofia, Faculty of Physics, 5 James Bourchier Blvd., 1164 Sofia, Bulgaria
[2] Department of Applied Physics, Technical University, 8 Kliment Ohridski Blvd., 1000 Sofia, Bulgaria
ln@phys.uni-sofia.bg

(Submitted on 15.10.2019. Accepted on 06.02.2020)

Abstract. The probability density function of column density (N-pdf) is an important indicator for understanding of physics and evolution of molecular clouds (MCs) in star-forming regions. Some N-pdfs derived from observational and numerical works could be decomposed to a lognormal part and a power-law tail (PLT) at their high-density ends. Recently, Veltchev et al. 2019 suggested a new approach for PLT extraction, which is not based on additional assumptions about the other parts of the distribution. In this paper we test the reliability of their method and its sensitivity to the chosen region, by use of numerical simulations of evolving giant MCs on galactic scales from the SILCC project. We found that the low-density gas outside the main filaments of the giant MCs does not contribute to the PLT range. The PLT of the N-pdf of molecular gas does not match the theoretical expectations for gravitational contraction – probably due to the complex chemical evolution and dynamics of MCs.

Key words: interstellar medium, star formation regions, data analysis, statistical methods, probability density distribution

Introduction

Molecular gas in galaxies tends to be organized into discrete clouds, called molecular clouds (MCs). MCs have complex shapes and internal structure; they are often highly filamentary and clumpy while most of their mass is contained in low-density fragments. Numerical simulations show that MCs form from interstellar warm atomic gas that is compressed by supersonic flows and cools down rapidly due to non-linear thermal instabilities, reaching temperatures $10 - 30$ K, number densities $n \sim 100$ cm^{-3} and turbulent velocity Mach numbers $\mathcal{M} \sim 20 - 30$ (for review, see MacLow & Klessen 2004, Vázquez-Semadeni 2010). Stars are born at a later evolutionary stage of MCs, when self-gravity in the cloud takes slowly over and local gravitational instabilities lead to collapse, fragmentation and formation of protostellar cores of densities $n \gtrsim 10^4 - 10^5$ cm^{-3}.

Main topic in the theory of star formation is the morphological and kinematical evolution of MCs. Recent scenarios of cloud formation suppose major contribution of supersonic turbulence which is ubiquitous in the interstellar medium. Numerical simulations show that driven turbulence at a given scale L is fully developed at about one crossing time $t_{\rm cr}(L)$ and saturated at $\sim 1.5t_{\rm cr}$ when a steady state is achieved (Passot et al. 1995; Federrath, Klessen & Schmidt 2008; Federrath et al. 2010). As an initial point of cloud evolution one takes usually a few crossing times which corresponds to a few Myr for clouds with effective sizes $1 - 10$ pc (Elmegreen 2000). On timescales ~ 10 Myr gravity starts to play an essential role in

the global evolution of the cloud (Vázquez-Semadeni et al. 2007, Vázquez-Semadeni 2010).

The cloud evolution could be traced either through the physical parameters of local substructures (clumps, cores) or in terms of indicators of general cloud structure. An increasingly used diagnostic tool to study the general structure is the probability density function (pdf). At evolutionary stage characterized by fully developed turbulence, the turbulent flows generate complex nets of gas condensations, leading to a lognormal probability distribution of mass density:

$$p(s)\,ds = \frac{1}{\sqrt{2\pi\sigma^2}} \exp\left[-\frac{1}{2}\left(\frac{s - s_{\rm mean}}{\sigma}\right)^2 \right] ds \ , \tag{1}$$

where $s = \ln(\rho/\rho_0)$, ρ_0 is the mean density in the considered volume and the standard deviation (stddev) σ is related to the peak position by:

$$s_{\rm mean} = -\frac{\sigma^2}{2} \ . \tag{2}$$

As the role of self-gravity in the MC evolution increases, the originally lognormal pdf of mass density (ρ-pdf) undergoes a gradual change. It develops a power-law tail (PLT) with a negative slope at its high-density end, as verified from many numerical simulations (e.g., Klessen 2000, Kritsuk, Norman & Wagner 2011, Collins et al. 2012, Federrath & Klessen 2012, 2013, Burkhart, Stalpes & Collins 2017). From the perspective of observations, one could derive and investigate the probability distribution of *column* density (N-pdf). It turns out to be morphologically analogous to the ρ-pdf; N-pdfs in star-forming clouds could be decomposed to a lognormal part and a PLT at their high-density ends (Schneider et al. 2013, Pokhrel et al. 2016). This is confirmed through numerical studies of contracting turbulent clouds (e.g., Ballesteros-Paredes et al. 2011, Federrath & Klessen 2013, Körtgen et al. 2019). The functional form of the developed PLT is:

$$p(s) = A\exp(ns) = A\exp(n\ln(N/N_0)) = A(N/N_0)^n \tag{3}$$

In the course of further evolution, the slope of the PLT in the ρ-pdf (Girichidis et al. 2014) and in the N-pdf (Veltchev et al. 2019; hereafter, V19) gets slowly shallower, tending toward a constant value. The main part of the N-pdf retains its (quasi-)lognormal shape while the deviation point (DP) from the lognormal fit shifts to lower values (Fig. 1).

However, the decomposition of N-pdfs in star-forming clouds to a lognormal bf part around the distribution peak and a PLT bf at the high-density end is not straightforward. There is an ongoing debate whether the lognormal part is clearly recognizable from observations (Lombardi, Alves & Lada 2015, Alves, Lombardi & Lada 2017) and can be extracted reliably. Another issue is that the two fitting functions are interdependent. If one assumes that the main N-pdf part is lognormal, the resulting DP and PLT slope depend on the lognormal parameters. Hence we need an

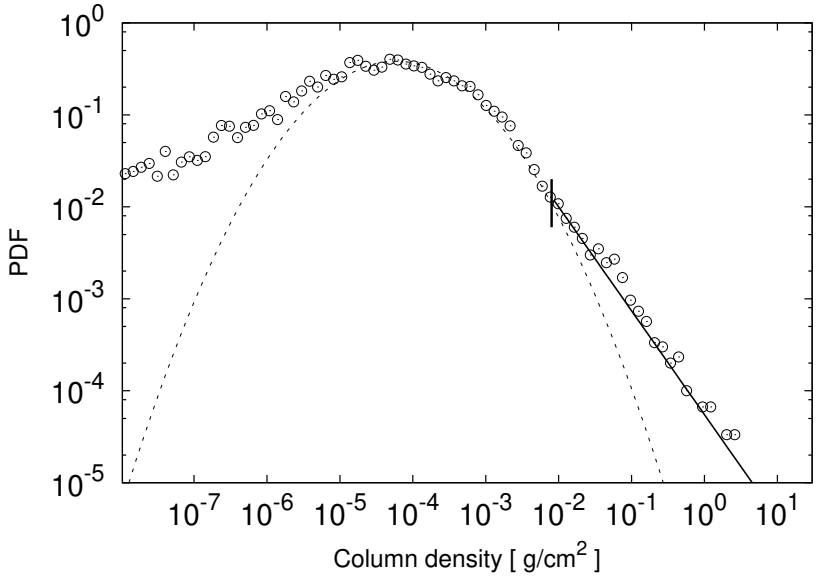

Fig. 1. Column density PDF of evolved molecular clouds: the distribution of H_2 in the whole SILCC cube at $t = 13.9$ Myr is taken for example. The main part is fitted by lognormal function (dashed; see eq. 1). The point of deviation (DP; vertical tick mark) and the power-law fit of the tail (PLT; solid line) are plotted.

approach to extract the PLT on minimal assumptions about the rest of the column-density distribution. Such was recently suggested by V19, based on the mathematical method BPLFIT (Virkar & Clauset 2014) which evaluates the possible PLT of an arbitrary distribution, without any assumptions about its other components.

Hereafter, we label the approach of V19 *adapted* BPLFIT *method* and this paper sets further steps toward its elaboration. Our aims are as follows: i) to probe the reliability of the method through comparison to a similar technique applied to unbinned data; ii) to investigate the possible dependence of the BPLFIT output on the selected region for study. Section 1 contains information on the used high-resolution data from the SILCC simulations. We present briefly the adapted BPLFIT method in Section 2. The results from our study are commented in Section 3 and summarized in the Conclusions.

1. Numerical Data

The used data set is part of simulations from the SILCC (Simulating the Life Cycle of Molecular Clouds) project (Walch et al. 2015, Girichidis et al. 2016). They use the hydrodynamical code FLASH (Fryxell et al. 2000), include feedback effects and trace the evolution of giant MCs in a galactic

environment. The scales covered range from 500 pc down to 0.12 pc. The simulation box with size $0.5 \times 0.5 \times \pm 5$ kpc^3 contains initially homogeneous strata of gas with decreasing density along the Z axis. The total gas surface density is $\Sigma_{\rm gas} = 10 {\rm M}_\odot {\rm pc}^{-2}$, hence total mass in the box is $2.5 \times 10^6 {\rm M}_\odot$. The gas is initially purely atomic, at rest, and follows a Gaussian distribution with a scale height of 30 pc. Gravitational effects are included, accounting for the stellar component of the galaxy by use of an external potential, which is implemented as an isothermal sheet with a stellar surface density of $30 {\rm M}_\odot {\rm pc}^{-2}$ (for more details, see Seifried et al. 2017, Girichidis et al. 2018). The star-formation efficiency in the used SILCC simulations is set constant in time which serves to estimate – combined with an assumption on the initial stellar mass function – the fraction of formed supernovae (SNe). The latter are let to explode at a constant rate of 15 Myr^{-1}.

To identify regions of giant MCs, the evolution of the gas was first followed for about 50 Myr (at a maximum resolution of $\Delta x = 3.9$ pc) and then the simulations are restarted at $t = 11.9$ Myr, progressively increasing the adaptive refinement up to a maximum resolution of $\Delta x = 0.12$ pc. In this paper we study the range of evolutionary times from 13.4 Myr to 16 Myr.

2. Methods

The predecessor of the bPlfit method is Plfit, proposed by Clauset, Shalizi & Newman (2009) "to discern and quantify power-law behaviour in empirical data". It operates with unbinned data and hence avoids any subjectivity at the PLT extraction due to the choice of binning size. The approach derives a power law fit of the data $p(x) \propto x^{-\alpha}$ above a chosen lower limit $x_{\rm min}$, using the Kolmogorov-Smirnov goodness-of-fit statistics. The procedure does not rule out that other (non-power-law) functions might better fit the observed distribution – it simply derives the range and the slope of the best possible power-law fit. This raises the issue whether the PLT extraction is reliable in case the main pdf part is lognormal and the lognormal wing at its high-density end is hardly distinguishable from a power-law function. The problem was studied in V19 (see Appendix B there) by use of analytical ρ-pdfs which are combinations of a lognormal function and a PLT. It turns out that the PLT slopes (steep or shallow) are derived with a high average accuracy, whereas the typical deviation of the DP from the real value is between 1 and 4 bins. We also performed additional tests on analytical ρ-pdfs with a very wide lognormal part, which mimic hydrodynamical simulations with compressive turbulent forcing (B. Körtgen, private communication), with similar results: uncertainty of the slope up to several dex and of the DP up to 4 bins. Hence the adapted bPlfit method can be deemed as reliable independent of the parameters of the lognormal pdf part.

Plfit works with unbinned data given that the data points are less than $\sim 10^5$ due to purely technical limitations. To deal with high-resolution maps of MCs or with large datasets from numerical simulations, one needs a different technique. To this end, a revised version of the method for binned distributions (Virkar & Clauset 2014) could be applied. This new method

is called bPLFIT and does not depend on assumptions about the binning scheme and is applicable to linear, logarithmic and arbitrary bins. V19 suggest an adapted bPLFIT method to extract *average* parameters of PLT, based on a large enough set of binnings of one and the same ρ-pdf/N-pdf. The procedure is described in details in V19. In this paper, the average PLT parameters are obtained through averaging over PDFs with 10 to 150 bins, adopting 8 bins as a minimal span of the PLT.

3. Results

We trace the evolution of the N-pdf derived from column-density maps obtained by projection of the SILCC data cube along the axis perpendicular to the galactic plane ($z = 0$). Additional refinement was applied in two zones of high column density centered at (40 pc, 180 pc) and (140 pc, -120 pc) which helps to distinguish cloudy and filamentary structures (Fig. 2, top, and the zoomed boxes therein) with typical sizes of GMCs (~ 100 pc). We label these regions GMC 1 and GMC 2 and investigate the evolution of their N-pdfs for two indicators: the total gas and the molecular gas (H_2). Four rectangular frames encompassing the GMCs were selected. They are of increasing size and will be used to study the effect of region selection on the PLT parameters (Sec. 3.2).

Table 1. Selected frames in the regions of additional refinement

Frame	Bottom-left corner coordinates		Sides	
#	x_0 [kpc]	y_0 [kpc]	Δx [kpc]	Δy [kpc]
GMC 1				
1	0.000	0.150	0.105	0.090
2	0.000	0.130	0.124	0.110
3	0.000	0.100	0.145	0.140
4	0.000	0.075	0.145	0.165
GMC 2				
1	0.115	-0.140	0.075	0.065
2	0.110	-0.160	0.100	0.100
3	0.100	-0.160	0.115	0.110
4	0.100	-0.180	0.130	0.130

Both PLFIT and the adapted bPLFIT methods were applied to the N-pdf in GMC 1 and GMC 2. The chosen time span of the SILCC run is between 13.4 and 16 Myr, with a timestep of 0.5 Myr. The chosen lower time limit corresponds to the stage of emergence of a PLT in the N-pdf with slope $n \gtrsim -4$, i.e. clearly distinguishable from a lognormal wing. It turned out that the results for GMC 1 and GMC 2 do not differ substantially and therefore we present below only those for GMC 1.

3.1. On the reliability of the adapted bPLFIT method

An appropriate way to test the reliability of the adapted bPLFIT is to compare its output to that from PLFIT. Unfortunately, as mentioned in Sect. 2,

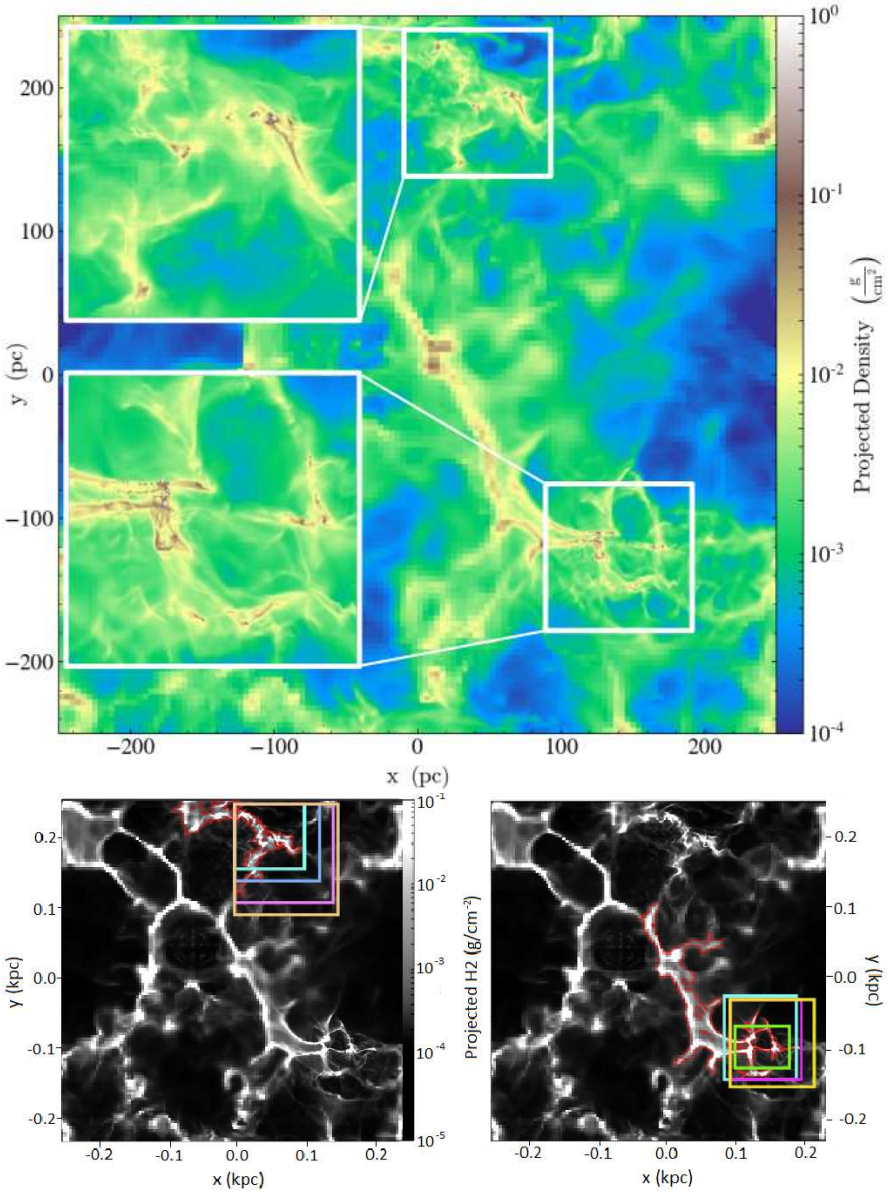

Fig. 2. Investigated regions from the SILCC run. *(Top:)* snapshot of the column-density field for the total gas at the end of the run; the zones of higher resolution, containing evolved GMCs, are zoomed in. *(Bottom:)* the same like the top panel but for H_2 only, with the plotted 4 rectangular frames and isocontours encompassing GMC 1 (left) and GMC 2 (right); see Table 1 and the text.

PLFIT is not applicable to very large sets of data (like in the whole SILCC cube), due to technical limitations. Therefore we consider only the regions of refinement to compare the output of both methods. Fig. 3 juxtaposes the derived PLT parameters for the total gas and H_2. The consistency is very good within the uncertainties of the BPLFIT procedure – especially for H_2. Considering the total gas, BPLFIT tends to underestimate the slope (typically by $0.1 - 0.3$ dex) and to yield higher values for the DP. This might be due to resolution effects which are increased by binning the high-density end of the N-pdf.

Generally, the slopes derived from the N-pdfs of the total gas and of H_2 behave differently. In the former case, the slope gets shallower in the course of the evolution (from small to large symbols in Fig. 3), reaching values ~ -1.70, while in the latter case it is remarkably constant, with an average value $\langle n \rangle(H_2)$ as low as $\simeq -1.20$. This finding hints at different physics accounting for the PLT formation and the evolution in dense cloud regions dominated by molecular gas. We comment on this issue in the next Section.

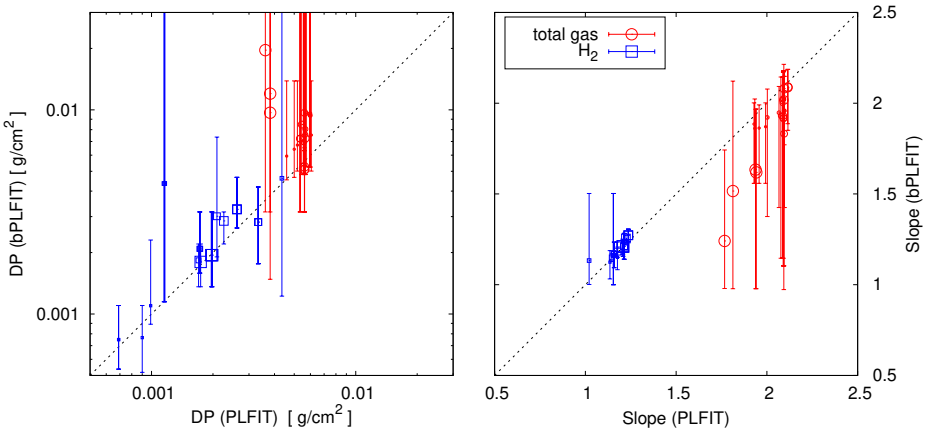

Fig. 3. Comparison between the PLT parameters in the chosen frames in GMC 1 obtained by PLFIT and BPLFIT. The symbol size is proportional to the evolutionary time: larger symbols correspond to later evolutionary stages. The identity line is plotted (dashed).

3.2. Dependence of the PLT parameters on the selected region

Now we address the issue how the PLT parameters in the N-pdf of molecular gas are influenced by the region of selection. Two different cases are analyzed (see Fig. 2): i) four rectangular frames which enclose the considered GMC and its diffuse vicinity; and ii) an isocontour with low-density cutoff $N_{\rm cut}$ below the average DP found from PLT analysis of the N-pdfs in the chosen frames. We want to address the 'problem of the last closed contour' formulated by Alves, Lombardi and Lada (2017; hereafter, ALL 17).

Those authors argue that the PLT is indeed the only reliably detectable part of the N-pdfs of *observed* clouds. The 'cloud' in observational studies is usually defined by introduction of a column density cutoff – this should cause simply an incompleteness in the low-density part of the resulting N-pdf and yield an apparently lognormal shape at lower densities while the DP of the PLT would practically coincide with the completeness limit (see Fig. 2 in ALL 17). Below we put this claim to test.

Case i) above is typical for observational studies of star-forming regions as one delineates a rectangular frame from the column-density map. However, the shape of the cloud is often irregular, asymmetric and filamentary and the choice of a frame may significantly affect the derived N-pdf. For instance, if some filamentary cloud structures are cut by the frame border this may lead to incompleteness of the N-pdf in the range of densities within those filaments. In Fig. 2 (top) one recognizes three main filaments in GMC 1 and an ensemble of clouds connected by thin filaments and spurs in GMC 2. Below we present the results on GMC 1.

All chosen frames encompass GMC 1, but cut off parts of its main filaments with mean column densities $N(\mathrm{H_2}) \lesssim 10^{-3}$ g cm^{-2} which is close to the average value in the entire cloud. Thus, one would expect that the N-pdf and the corresponding PLT will vary with the frame. However, as seen in Fig. 4 (left), the PLT parameters in all frames and at given evolutionary stage are very similar. This means that the gas of lower density outside the main filaments of GMC 1 does not contribute to the PLT range. The latter is defined by a mean $\langle \mathrm{DP} \rangle \sim 2 \times 10^{-3}$ g cm^{-2}$\sim 10^{21}$ cm^{-2}, which corresponds roughly to the critical value at which massive gas condensations become magnetically supercritical (Vazquez-Semadeni et al. 2011). This result possibly hints at the gravitational boundedness of the cloudy structures delineated by an isocontour of this value. On the other hand, the non-power-law parts of the N-pdfs in the considered frames (not shown) span many orders of magnitude in logdensity and extinction[3] A_V, which calls into question the claim of ALL 17 that the derived DPs should mark the completeness limits. To eliminate possible biases from the applied method, we delineate a region within an isocontour with $N_\mathrm{cut} = 4 \times 10^{-4}$ g cm^{-2} – a value which is: i) clearly below the found DPs so that BPLFIT would be able to distinguish a PLT from a non-power-law N-pdf part; and ii) less than an order of magnitude from the estimated DPs, which mimics the observational N-pdfs studied by ALL 17. The obtained PLT parameters in the isocontour region are very similar to the ones from the rectangular frames, although the region is larger than GMC 1 (cf. Fig. 2, bottom). In other words, the introduction of a column-density cut-off $N_\mathrm{cut} < \langle \mathrm{DP} \rangle$, corresponding to an isocontour which is not entirely enclosed in the considered cloud map, does not contribute to the PLT range in the N-pdf. This seems to be in agreement with the claim of ALL 17. A further step to confirm the result would be to use synthetic observations.

The right panel of Fig. 4 compares the evolution of the PLT parameters in the isocontour region with those from the N-pdf in the entire SILCC cube, taken from V19. Evidently, the uncertainties of the PLT parameters of the N-pdf in the whole SILCC cube are large due to contributions

[3] If one applies a constant ratio $N(\mathrm{H})/A_V$ [cm^{-2}]; e.g. Bohlin et al. 1978.

from different regions, (possibly) at different evolutionary stages. The general tendency is that the PLT gets shallower while the DP remains nearly constant, with variations within one order of magnitude (see also Fig. 6 in V19). Note that this shallowing is not due to evolution of the star-formation efficiency which is set to be constant in the SILCC runs (Sect. 1).

The slope from the isocontour does not change with the course of evolution and is close to unity, much less than expected from theoretical considerations of late evolutionary stage in self-gravitating clouds ($|n| \sim 2$; see Donkov et al. 2017, and references therein) and than the slopes refered to by ALL 17 in star-forming ($|n| \sim 2$) and diffuse clouds ($|n| \sim 4$). Steeper slopes are derived from the N-pdf of the whole SILCC cube (V19; cf. Fig. 4, right) but we warn that they might be affected by insufficient resolution at the high density end, in contrast to the regions of higher refinement studied in this paper. Our claim is that the N-pdf of molecular gas should not necessarily follow what one expects for the evolution of total gas from simple considerations of gravitational contraction – in view of the complex chemical evolution and dynamics of MCs (Vázquez-Semadeni 2010).

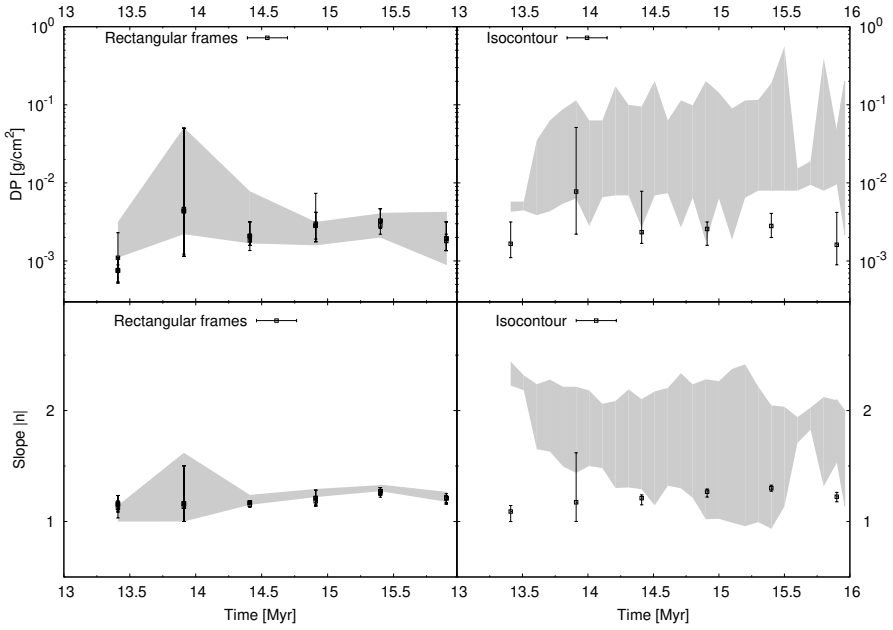

Fig. 4. Evolution of the PLT parameters derived through BPLFIT from the N-pdf of H_2 in selected regions within the refinement zone GMC 1 of the SILCC cube. *Left:* in rectangular frames, compared with those in the isocontour region (grey area; corresponding to the uncertainty range of the data in the right panel). *Right:* in an isocontour region with low-density cutoff $N_{\rm cut} = 2 \times 10^{-3}$ g cm^{-2}, compared with the evolution of the PLT parameters in the whole cube (taken from V19; grey area).

Conclusions

This work presents a study of the power-law tail (PLT) extracted from the probability density function of column-density (N-pdf) of simulated molecular clouds (MCs), at advanced stages of their evolution. We used numerical data from the SILCC project which include several refinement levels and construct a column-density map by projection of the data cube along the axis perpendicular to the galactic plane. Two giant MCs are seen in the refinement zones on this map and we apply to their N-pdfs two different approaches of PLT extraction: PLFIT (Clauset, Shalizi & Newman 2009) for unbinned data and the adapted BPLFIT (Veltchev et al. 2019) for binned distribution.

The extracted PLTs are characterized by two parameters: slope and deviation point (DP; i.e. the lower-density limit of the tail). The PLT evolution was followed in: i) four rectangular frames which enclose the considered giant MC and its diffuse vicinity; and ii) an isocontour defined by low-density cutoff $N_{\rm cut}$ less than to the average DP found from PLT analysis of the frames from case i). The results are as follows:

- The PLT parameters derived by use of the adapted BPLFIT method are in very good consistency with those from PLFIT. This is a confirmation that novel adapted BPLFIT technique is a reliable approach for extraction of PLTs.
- The PLT parameters in all rectangular frames and at given evolutionary stage are very similar. This means that the molecular gas of lower density outside the main filaments of the giant MCs does not contribute to the PLT range. The average DP roughly coincides with the column density at which massive clumps become supercritical – which possibly hints at the gravitational boundedness of the cloudy structures delineated by an isocontour of this value.
- The slope from the isocontour remains nearly constant in time ($\gtrsim -1.2$) and is much less than expected from theory of self-gravitating clouds ($n \sim -2$) and than the slopes from observations of star-forming as well diffuse clouds. Our explanation is that the PLT of the N-pdf of molecular gas should not necessarily follow what one expects for the evolution of total gas from simple considerations of gravitational contraction – in view of the complex chemical evolution and dynamics of MCs (Vázquez-Semadeni 2010).

Acknowledgments: We thank the anonymous referee for the critical reading of the manuscript and for the insightful comments which helped us to improve this paper. L.M. acknowledges support by the program "Young scientists and PhD students" approved by the Government of Republic of Bulgaria, Grant # 70-06-181/21.03.2019 and also Ministry of Education and Science of the Republic of Bulgaria, National RI Roadmap Project DO1-277/16.12.2019. The authors are grateful to Philipp Girichidis who kindly provided us with the numerical data from a SILCC run with high-resolution in selected areas and to Bastian Körtgen for the discussion on his simulations with compressed turbulent forcing.

References

Alves, J., Lombardi, M., Lada, C., 2017, A&A, 606, L2 (ALL 17)
Ballesteros-Paredes, J., Vázquez-Semadeni, E., Gazol, A., Hartmann, L., Heitsch, F., Colín, P., 2011, MNRAS, 416, 1436
Bohlin, R., Savage, B., Drake, J., 1978, ApJ, 224, 132
Burkhart, B., Stalpes, K., Collins, D., 2017, ApJ, 834, L1
Clauset, A., Shalizi, C. R., Newman, M. E. J., 2009, SIAM Rev., 51, No. 4, 661
Collins, D., Kritsuk, A., Padoan, P., Li, H., Xu, H., Ustyugov, S., Norman, M., 2012, ApJ, 750, 13
Donkov, S., Veltchev, T., Klessen, R. S., 2017, MNRAS, 466, 914
Elmegreen, B., 2000, ApJ, 530, 277
Federrath, C., Klessen, R. S., 2012, ApJ, 761, 156
Federrath, C., Klessen, R. S., 2013, ApJ, 763, 51
Federrath, C., Klessen, R., Schmidt, W., 2008, ApJ, 688, L79
Federrath, C., Roman-Duval, J., Klessen, R., Schmidt, W., Mac Low, M.-M., 2010, A&A, 512, 81
Fryxell, B., Olson, K., Ricker, P. et al. 2000, ApJS, 131, 273
Girichidis, P., Konstandin, L., Whitworth, A. P., Klessen, R. S., 2014, ApJ, 781, 91
Girichidis, P., Seifried, D., Naab, T., Peters, T., Walch, S., Wünsch, R., Glover, S. C. O., Klessen, R. S., 2018, MNRAS, 480, 3511
Girichidis, P., Walch, S., Naab, T., Gatto, A., Wünsch, R., Glover, S. C. O., Klessen, R. S., Clark, P. C., et al., 2016, MNRAS, 456, 3432
Klessen, R. S., 2000, ApJ, 535, 869
Körtgen, B., Federrath, C., Banerjee, R., 2019, MNRAS, 482, 5233
Kritsuk, A., Norman, M., Wagner, R., 2011, ApJL, 727, L20
Lombardi, M., Alves, J., Lada, C. J., 2015, A&A, 576, L1
MacLow, M.-M., Klessen, R. S., 2004, Rev. Modern Phys., 76, 125
Passot, T., Vázquez-Semadeni, E., & Pouquet, A., 1995, ApJ, 455, 536
Pokhrel, R., Gutermuth, R., Ali, B., Megeath, T., Pipher, J., Myers, P., Fischer, W. J., Henning, T., et al., 2016, MNRAS, 461, 22
Schneider, N., André, Ph., Könyves, V., Bontemps, S., Motte, F., Federrath, C., Ward-Thompson, D., Arzoumanian, D., et al. 2013, ApJ, 766, L17
Seifried, D., Walch, S., Girichidis, P., Naab, T., Wünsch, R., Klessen, R. S., Glover, S. C. O., Peters, T., Clark, P., 2017, MNRAS, 472, 4797
Vázquez-Semadeni, E., 2010, in Kothes R., Landecker T. L., Willis A. G., eds, ASP Conf. Ser. Vol. 438, *The Dynamic Interstellar Medium: A Celebration of the Canadian Galactic Plane Survey*. Astron. Soc. Pac., San Francisco, p. 83
Vázquez-Semadeni, E., Banerjee, R., Gómez, G., Hennebelle, P., Duffin, D., Klessen, R. S., 2011, MNRAS, 414, 2511
Vázquez-Semadeni, E., Gómez, G., Jappsen, A., Ballesteros-Paredes, J., González, R., Klessen, R. S., 2007, ApJ, 657, 870
Veltchev, T., Girichidis, Ph., Donkov, S., Schneider, N., Stanchev, O., Marinkova, L., Seifried, S., Klessen, R. S., 2019, MNRAS, 489, 788 (V19)
Virkar, Y., Clauset, A., 2014, Annals of Appl. Stat., vol. 8, No. 1, 89 (arXiv:1208.3524)
Walch, S., Girichidis, P., Naab, T., Gatto, A., Glover, S. C. O., Wünsch, R., Klessen, R. S., Clark, P. C., et al., 2015, MNRAS, 454, 238